Photoelectrochemistry Hot Paper

DOI: 10.1002/anie.201408375

Forming Buried Junctions to Enhance the Photovoltage Generated by Cuprous Oxide in Aqueous Solutions**

*Pengcheng Dai, Wei Li, Jin Xie, Yumin He, James Thorne, Gregory McMahon, Jinhua Zhan, and Dunwei Wang**

Abstract: *Whereas wide-bandgap metal oxides have been extensively studied for the photooxidation of water, their utilization for photoreduction is relatively limited. An important reason is the inability to achieve meaningful photovoltages with these materials. Using Cu_2O as a prototypical photocathode material, it is now shown that the photovoltage barrier can be readily broken by replacing the semiconductor/water interface with a semiconductor/semiconductor one. A thin ZnS layer (ca. 5 nm) was found to form high-quality interfaces with Cu_2O to increase the achievable photovoltage from 0.60 V to 0.72 V. Measurements under no net exchange current conditions confirmed that the change was induced by a thermodynamic shift of the flatband potentials rather than by kinetic factors. The strategy is compatible with efforts aimed at stabilizing the cathode that otherwise easily decomposes and with surface catalyst decorations for faster hydrogen evolution reactions. A combination of NiMo and CoMo dual-layer alloy catalysts was found to be effective in promoting hydrogen production under simulated solar radiation.*

Among all sources of renewable energy, solar energy is the only one that can be utilized on a scale comparable to that of our ever-growing needs.[1,2] Its utilization, however, must address challenges associated with its diurnal and intermittent nature. In principle, this issue can be addressed by carrying out water splitting reactions using methods such as photoelectrochemistry (PEC) that harvest and store solar energy in chemical bonds.[3,4] To successfully carry out these reactions, we need high-performance photoelectrode materials for both the oxidation (anode) and reduction (cathode) reactions.[5–7] Based on cost and stability considerations, metal oxides are attractive photoelectrode candidates. Whereas significant research efforts have been devoted to studying oxides as photoanodes,[5,8–14] comparably little has been done on using metal oxides as photocathodes. This is in part due to the fact that p-type metal oxides are relatively rare compared to n-type ones. The lack of research on oxide photocathodes is also a result of bandgap matching considerations for dual absorber systems.[15] As metal oxides often feature wide bandgaps (>2 eV), studies on oxide photocathodes will be of practical value only if stable narrow-bandgap (ca. 1 eV) photoanodes are available. Previously, this has been a challenge. Recent developments in stabilizing narrow-bandgap photoanodes, such as those made of silicon, have changed this situation.[6,16] It is within this context that Cu_2O, a non-toxic, low-cost p-type semiconductor with a band gap of 2 eV, stands out as the photocathode of choice.[17,18] Indeed, Cu_2O has received sustained interest for over a decade, and prior research has primarily been focused on increasing the photocurrent and stabilizing it in water under reducing conditions.[18–20] The important question of how to increase its photovoltage has not been addressed. Limited by the difference between the Fermi level of Cu_2O (-5.19 eV)[18,21] and the hydrogen evolution potential (-4.50 eV at pH 0), the highest photovoltage measured on Cu_2O in H_2O was 0.6 V,[20,22] which is lower than what is needed to match the relatively low photovoltage by a narrow-bandgap photoanode. When characterized in a non-aqueous system, a photovoltage of up to 0.8 V has been measured on Cu_2O,[23] suggesting that there is still much room for improvement in terms of photovoltage generation by Cu_2O in H_2O. Herein we show a strategy to address this issue. By substituting the Cu_2O/H_2O interface with a Cu_2O/ZnS junction, we were able to readily increase the photovoltages by up to 20%. Importantly, our approach is compatible with treatments aimed at stabilizing Cu_2O, for example, with TiO_2 grown by atomic layer deposition (ALD).[18–20] The system is shown to perform well in conjunction with catalysts based on earth-abundant elements (e.g., NiMo and CoMo).[24,25]

The governing principle of metal-oxide-based PEC water splitting is the effect known as band edge pinning, in which the band edge positions are pinned relative to the H_2O redox potential. The degree of band bending, and hence the maximum achievable photovoltage, is defined by the difference between the flatband potential (V_{fb}) and the chemical potential of the targeted reaction in H_2O (hydrogen evolution reaction, or HER, in the present study).[26,27] In the case of

[*] P. Dai,[+] W. Li,[+] J. Xie, Y. He, J. Thorne, Dr. G. McMahon, Prof. Dr. D. Wang
Department of Chemistry
Merkert Chemistry Center, Boston College
2609 Beacon St., Chestnut Hill, MA 02467 (USA)
E-mail: dunwei.wang@bc.edu
P. Dai,[+] Prof. Dr. J. Zhan
Key Laboratory for Colloid and Interface Chemistry of Education Ministry, Shandong University
27 South Shanda Road, Jinan, Shandong, 250100 (P.R. China)
[+] These authors contributed equally to this work.

[**] This work is supported by the National Science Foundation (DMR 1055762). D.W. is an Alfred P. Sloan Fellow. J.Z. is supported by the National Basic Research Program of China (973 Program, 2013CB934301) and the National Natural Science Foundation of China (NSFC91023011). We are grateful for technical support from Xiahui Yao, Steve Shepard, and Lien-Yang Chou. We also thank David Bell for technical assistance with STEM at the Center for Nanoscale Systems (CNS).

Supporting information for this article is available on the WWW under http://dx.doi.org/10.1002/anie.201408375.

Cu_2O, the value is approximately 0.6 based on Fermi level data in vacuum. To break the barrier, we would need to shift the band edge positions, for example, by introducing surface dipoles. Although organic dipole molecules have been shown to work well for this purpose in dye-sensitized solar cells,[28,29] their utility in solar water-splitting devices is limited owing to their poor stabilities under harsh conditions. An alternative approach is based on the formation of buried solid/solid junctions. For this purpose, we require n-type semiconductors whose valence and conduction band edges are sufficiently negative. With a valence band maximum of −7.58 eV and a conduction band minimum of −3.90 eV,[30] ZnS stands out (Figure 1a). This approach is similar to decorating p-type Si with n^+ players, which was described by Lewis et al.[31] It also aligns with our approach to form homojunctions on hematite for water oxidation.[11] The key to its success is to keep the top layer thin because the primary role of the n-type layer is to increase band bending within the p-type photocathode. Opposite band bending may develop in a thicker n-type layer, trapping electrons to negatively influence the functionality of the device (see the Supporting information).

One particular weakness of Cu_2O that has received significant attention is its instability in H_2O. Often, Cu_2O undergoes reduction to yield Cu instead of H_2 when used as the photocathode. To address this issue, we used ALD-grown TiO_2 as a protection layer (ca. 100 nm).[18–19,32] Catalysts were used to promote the HER. The overall material structure is shown in Figure 1b. The structural details are presented in Figure 2a, where scanning electron microscopy (SEM) data is presented. A conformal coverage of Cu_2O by the TiO_2 overlayer is afforded by the ALD growth (Figure 2a). The ZnS decoration, owing to its thinness, is not pronounced at the magnification used in Figure 2a. Scanning transmission electron microscopy (STEM) was therefore carried out to probe the elemental composition (Figure 2b).

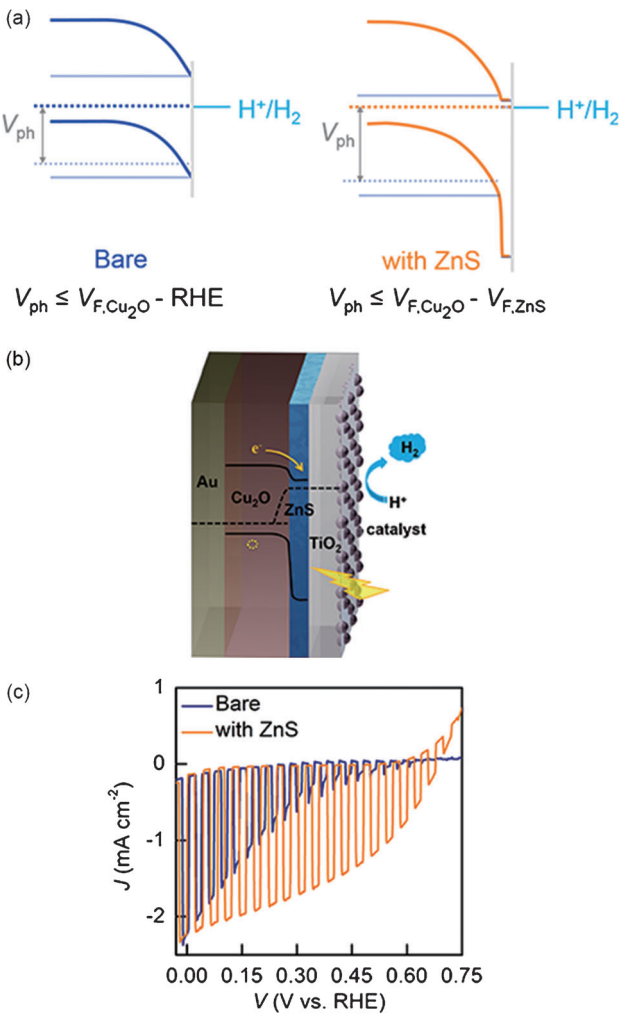

Figure 1. Replacing the Cu_2O/H_2O interface with Cu_2O/ZnS junctions readily improves photovoltage generation by Cu_2O. a) A schematic representation of the band structures shows how the addition of ZnS moves the band edge position in the positive direction for a more substantial built-in field. b) Three-dimensional perspective view of the material structure, the TiO_2 protective layer, and the surface HER catalysts. c) Polarization curves of bare Cu_2O (Cu_2O/TiO_2/Pt) and Cu_2O/ZnS (Cu_2O/ZnS/TiO_2/Pt) in KH_2PO_4 buffer solution (0.2 M, pH 7), under chopped AM 1.5 illumination.

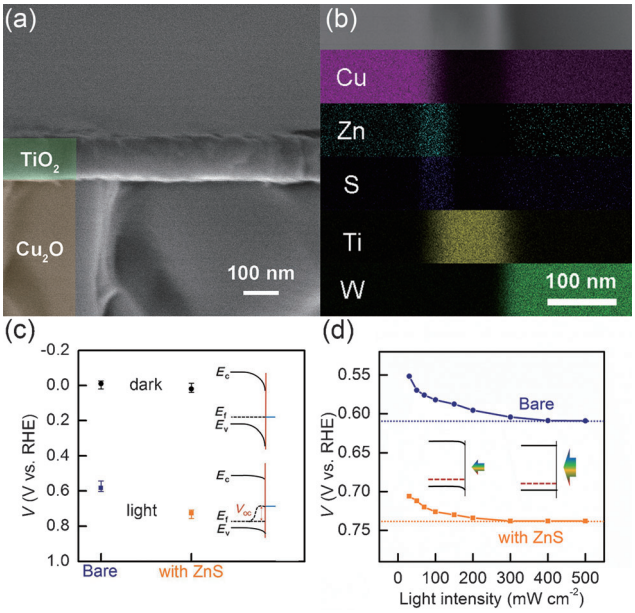

Figure 2. Microstructures of the Cu_2O/ZnS/TiO_2 photocathode and OCP measurements. a) Scanning electron micrograph showing a conformal overlayer of TiO_2 on Cu_2O. b) Scanning transmission electron micrographs with selected filters revealing the elemental composition of the different layers across the top image. From top to bottom: overall view, Cu distribution, Zn distribution, S distribution, Ti distribution, and W distribution. W was deposited as a protection layer by focused ion beam milling. c) Compared with bare Cu_2O, Cu_2O/ZnS shows a more positive open circuit potential under illumination, indicating a positive shift of its V_{fb} value, as shown in Figure 1a. d) The true V_{fb} values of both bare Cu_2O (blue) and Cu_2O/Zn (orange) are probed by increasing the illumination intensity.

In principle, the design shown in Figure 1a and b should work for any HER catalyst. In practice, the performance of the photoelectrode is sensitive to the nature of the catalyst/semiconductor interface. To focus on the effect of the ZnS decoration on the performance of the Cu_2O, we will next present results that were obtained with the best performing

HER catalyst, Pt nanoparticles. Afterwards, we will show that similar results can be obtained with more earth-abundant catalysts, such as NiMo and CoMo alloys.

Our first task was to confirm that the application of ZnS indeed increases the degree of band bending within Cu_2O. Steady-state current–voltage measurements are the most popular technique to evaluate the performance of photoelectrodes. As shown in Figure 1c, the difference between Cu_2O with and without ZnS decoration was obvious. If we define the turn-on voltage as the potential where we first observed photocurrent under chopped light, a V_{on} of 0.6 V was obtained for the Cu_2O photoelectrode. When ZnS was present, a V_{on} of 0.72 V was measured. Nevertheless, the steady-state current measurements are not suitable for quantitative analysis because the change in V_{on} may be influenced either by thermodynamic (increase in band bending) or kinetic (reduction in kinetic overpotentials) factors or both.[33,34] To obtain information specific to band bending, we previously developed an open-circuit potential (OCP) measurement technique that permits us to probe the resting potentials at zero net exchange current densities, where kinetic factors do not play a role.[10,34] As shown in Figure 2c, in the absence of illumination, the resting potential should be equal to that of the HER, namely 0 V (vs. RHE, reversible hydrogen electrode). We caution that it is critical to establish a reversible HER at or near standard conditions to measure 0 V (vs. RHE). It means that the solution should be saturated with H_2 gas, and the presence of a HER catalyst is necessary. Otherwise, erroneous OCP values are obtained in the dark (see the Supporting Information). Once the conditions outlined above were met, the results presented in Figure 2c were highly reproducible. Under illumination, photoexcited electrons populate the conduction band on or near the surface, splitting the quasi-Fermi levels of electrons and holes, which leads to the flattening of the band. The measured OCP tracks the Fermi level of the majority carriers (holes in the case of p-type Cu_2O). The Fermi level of the holes is expected to move in the positive direction under illumination, and the OCP difference in the dark and under illumination describes the photovoltage generated by the semiconductor/water interface. Indeed, Cu_2O without ZnS gave a photovoltage of 0.58 ± 0.04 V, which is consistent with literature reports. The presence of ZnS modifies the Cu_2O/H_2O interface and increases the degree of band bending. A greater photovoltage (0.73 ± 0.03 V) was correspondingly measured (Figure 2c). It should be noted that Al-doped ZnO (AZO) has previously been used to form p–n^+ junctions on Cu_2O. Whereas the charge collection could be improved, no obvious effect on the photovoltage was reported.[18] The degenerate doping and the positions of the Fermi level relative to the band edges in the case of AZO may be reasons for the apparent differences.

The degree of quasi-Fermi level splitting and hence the measured photovoltage are expected to depend on the light intensity.[35] Under relatively weak illumination, the band is partially flattened; the degree of band flattening follows the light intensity with an exponential relationship and reaches saturation under strong illumination owing to saturation of the states available for minority carrier densities. We could indeed observe this trend (Figure 2d). The results offer us confidence that the OCP measurement as discussed above is a reliable technique to probe the degree of band bending without the influence of kinetic factors. Furthermore, it is noteworthy that the OCP results are not sensitive to the pH value (see the Supporting Information), further highlighting the validity of the technique.

As the surfaces of both photoelectrodes (with and without ZnS decoration) are decorated with the same HER catalysts (Pt nanoparticles), the charge transfer kinetics across the photoelectrode/water interface may be regarded as comparable. Under such limiting conditions, we may quantify the V_{on} values by steady-state measurements more precisely following the Butler method.[36] To do so, monochromic illumination is required so that the light absorption coefficient of the photoelectrode is defined more accurately. A V_{on} value of 0.59 V was measured for Cu_2O; with ZnS, the value increased to 0.71 V (Figure 3a), which corresponds to an anodic shift of 0.12 V.

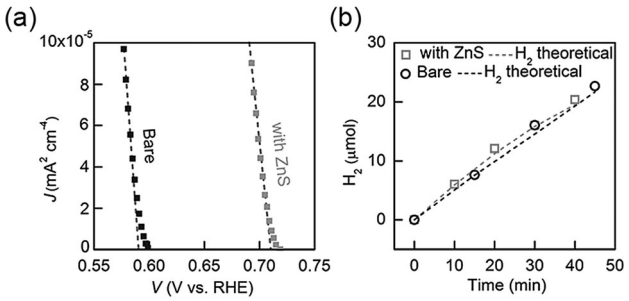

Figure 3. Characterization of Cu_2O/ZnS performance. a) Butler plot demonstrating the more positive V_{fb} value for Cu_2O/ZnS. b) Amount of hydrogen evolved by Cu_2O based photocathodes as detected by mass spectrometry, matching the number of charges measured. The theoretical line was calculated according to Faraday's law of electrolysis: $N_{H_2} = \frac{1}{2} N_{Charge}$.

Collectively, the OCP measurements, the steady-state characterization under white light, and the Butler quantification under monochromic light support the hypothesis that the application of ZnS increases the degree of band bending within Cu_2O from 0.59 V to 0.71 V. Whereas the absolute increase (0.12 V) may seem modest, it is the first time that a photovoltage of greater than 0.6 V, the theoretical value based on the difference between the Fermi level of Cu_2O and the HER, has been measured and reported. This result highlights that there is indeed much to gain from Cu_2O, opening up possibilities of integrating this material with narrow-bandgap anodes stabilized by metal oxide protective layers. Lastly, we want to emphasize that the steady-state measurements (Figure 1c and 3a) indeed correspond to the HER. By detecting the reaction product, H_2, and by comparing the amount formed with the number of charges passed through, we obtained a Faradaic efficiency close to 100% (Figure 3b).

Before the system shown in Figure 1 can be used for practical applications, there are still two issues that deserve further discussion. The first issue concerns the ALD-grown TiO_2 layer. Despite its thickness, the presence of this layer

does not seem to alter the nature of the Cu_2O/H_2O interface in any significant fashion. Similar results have been independently obtained by Grätzel et al.[19] on ALD-grown TiO_2 and by Chorkendorff et al.[32] on thermally grown TiO_2. It has been suggested that this may be due to the the coincidental alignment of the TiO_2 Fermi level with the HER. The understanding of the true electronic nature of the TiO_2 protection layer, however, requires additional research. It should be noted that the TiO_2 layer employed in our studies does not feature any intentional doping. Films that are thinner than 20 nm failed to provide adequate protection, and those thicker than 200 nm resulted in dramatically reduced photocurrent densities. Films of 100 nm offered the best performance in terms of stability and photocurrent densities (see the Supporting Information, Figure S9).

The second issue concerns the usage of Pt. There is a rapidly growing interest in replacing Pt with earth-abundant HER catalysts. New classes of compounds that are based on chalcogenides or phosphides have proven effective,[37] some of which have been employed in combination with Cu_2O for the photoelectrode reduction of H_2O.[20,38] As a proof of concept, we would like to demonstrate that the strategy presented herein is compatible with earth-abundant HER catalysts. For this purpose, we studied two Mo-based alloy systems, NiMo and CoMo nanoparticles, which have been shown to enable HER in neutral and basic solutions, with $Ni_{8.6}Mo$ and $Co_{37}Mo$ featuring η values of 200 mV and 170 mV, respectively, at $J = 100\ mA\,cm^{-2}$.[25] Interestingly, we found that whereas CoMo exhibited a better HER activity than that measured by Piron,[25] NiMo enabled greater photovoltages, as indicated by the more positive V_{on} value (Figure 4; see also the Supporting Information, Figure S10).

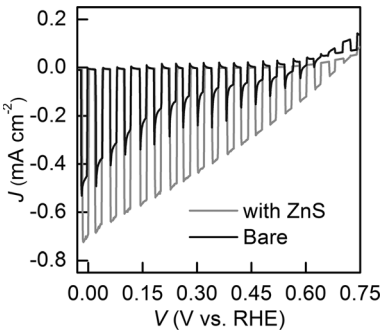

Figure 4. Polarization curves of bare Cu_2O (black) and Cu_2O/ZnS (gray), both modified with a NiMo/CoMo dual-layer catalyst, in KH_2PO_4 buffer solution (0.2 M, pH 7) under chopped AM 1.5 illumination.

We believe that the CoMo material produced in our studies is catalytically more active whereas the NiMo afforded a higher-quality interface with TiO_2. Inspired by the approach of Choi et al. to decorate $BiVO_4$ surfaces with FeOOH and NiOOH,[39] we applied dual-layer catalysts with NiMo as the underlayer and CoMo as the outer layer. In the absence of ZnS, a V_{on} of 0.61 V was measured, the corresponding J at HER was $0.47\ mA\,cm^{-2}$. When ZnS was present, the V_{on} increased to 0.73 V, and the J at HER also increased to $0.71\ mA\,cm^{-2}$. Clearly, optimization is still needed to obtain a performance comparable to that of Pt. Higher current densities have been achieved when nanoscale features are introduced to the Cu_2O substrate.[18,20] Nonetheless, to the best of our knowledge, the turn-on values are the highest that have been reported in the literature to date.

In conclusion, we have shown that a simple ZnS modification strategy can readily increase the photovoltage generated by Cu_2O in H_2O. This work addresses an important issue in photoelectrochemical water splitting. Whereas a dual-absorber system has widely been recognized as a promising configuration, the achievement of large photovoltages from wide-bandgap top layers constitutes a significant challenge. Often the achievable photovoltage is limited by the difference between the flatband potential and the electrochemical potential of the solution, compounded by partial or complete band edge unpinning effects. Our results suggest that modifying the semiconductor/H_2O interface is a strategy that can be used to enable the construction of photoelectrode materials with desired properties. Although more investigations are still required to improve photovoltage and photocurrent with promising materials such as Cu_2O, new doors have been opened to enable the development of practical solar water splitting devices that are based on earth-abundant, stable metal oxide semiconductors.

Received: August 19, 2014
Revised: September 5, 2014
Published online: October 3, 2014

Keywords: cuprous oxide · hydrogen · photoelectrochemistry · solar energy conversion · water splitting

[1] N. S. Lewis, D. G. Nocera, *Proc. Natl. Acad. Sci. USA* **2006**, *103*, 15729 – 15735.
[2] M. Graetzel, *Acc. Chem. Res.* **1981**, *14*, 376 – 384.
[3] M. G. Walter, E. L. Warren, J. R. McKone, S. W. Boettcher, Q. Mi, E. A. Santori, N. S. Lewis, *Chem. Rev.* **2010**, *110*, 6446 – 6473.
[4] O. Khaselev, J. A. Turner, *Science* **1998**, *280*, 425 – 427.
[5] K. Sivula, F. Le Formal, M. Grätzel, *ChemSusChem* **2011**, *4*, 432 – 449.
[6] M. J. Kenney, M. Gong, Y. Li, J. Z. Wu, J. Feng, M. Lanza, H. Dai, *Science* **2013**, *342*, 836 – 840.
[7] P. Dai, J. Xie, M. T. Mayer, X. Yang, J. Zhan, D. Wang, *Angew. Chem. Int. Ed.* **2013**, *52*, 11119 – 11123; *Angew. Chem.* **2013**, *125*, 11325 – 11329.
[8] M. T. Mayer, C. Du, D. Wang, *J. Am. Chem. Soc.* **2012**, *134*, 12406 – 12409.
[9] M. T. Mayer, Y. Lin, G. Yuan, D. Wang, *Acc. Chem. Res.* **2013**, *46*, 1558 – 1566.
[10] X. Yang, C. Du, R. Liu, J. Xie, D. Wang, *J. Catal.* **2013**, *304*, 86 – 91.
[11] Y. Lin, Y. Xu, M. T. Mayer, Z. I. Simpson, G. McMahon, S. Zhou, D. Wang, *J. Am. Chem. Soc.* **2012**, *134*, 5508 – 5511.
[12] K. Sivula, F. L. Formal, M. Grätzel, *Chem. Mater.* **2009**, *21*, 2862 – 2867.
[13] S. D. Tilley, M. Cornuz, K. Sivula, M. Grätzel, *Angew. Chem. Int. Ed.* **2010**, *49*, 6405 – 6408; *Angew. Chem.* **2010**, *122*, 6549 – 6552.
[14] A. Braun, K. Sivula, D. K. Bora, J. Zhu, L. Zhang, M. Grätzel, J. Guo, E. C. Constable, *J. Phys. Chem. C* **2012**, *116*, 16870 – 16875.
[15] J. R. Bolton, S. J. Strickler, J. S. Connolly, *Nature* **1985**, *316*, 495 – 500.

[16] S. Hu, M. R. Shaner, J. A. Beardslee, M. Lichterman, B. S. Brunschwig, N. S. Lewis, *Science* **2014**, *344*, 1005 – 1009.
[17] M. Hara, T. Kondo, M. Komoda, S. Ikeda, J. N. Kondo, K. Domen, K. Shinohara, A. Tanaka, *Chem. Commun.* **1998**, 357 – 358.
[18] A. Paracchino, V. Laporte, K. Sivula, M. Grätzel, E. Thimsen, *Nat. Mater.* **2011**, *10*, 456 – 461.
[19] A. Paracchino, N. Mathews, T. Hisatomi, M. Stefik, S. D. Tilley, M. Grätzel, *Energy Environ. Sci.* **2012**, *5*, 8673 – 8681.
[20] C. G. Morales-Guio, S. D. Tilley, H. Vrubel, M. Grätzel, X. Hu, *Nat. Commun.* **2014**, *5*, 3509.
[21] L. I. Bendavid, E. A. Carter, *J. Phys. Chem. B* **2013**, *117*, 15750 – 15760.
[22] S. D. Tilley, M. Schreier, J. Azevedo, M. Stefik, M. Graetzel, *Adv. Funct. Mater.* **2014**, *24*, 303 – 311.
[23] C. Xiang, G. M. Kimball, R. L. Grimm, B. S. Brunschwig, H. A. Atwater, N. S. Lewis, *Energy Environ. Sci.* **2011**, *4*, 1311 – 1318.
[24] J. R. McKone, B. F. Sadtler, C. A. Werlang, N. S. Lewis, H. B. Gray, *ACS Catal.* **2013**, *3*, 166 – 169.
[25] C. Fan, D. L. Piron, A. Sleb, P. Paradis, *J. Electrochem. Soc.* **1994**, *141*, 382 – 387.
[26] J. Bisquert, P. Cendula, L. Bertoluzzi, S. Gimenez, *J. Phys. Chem. Lett.* **2013**, *5*, 205 – 207.
[27] C. Du, M. Zhang, J.-W. Jang, Y. Liu, G.-Y. Liu, D. Wang, *J. Phys. Chem. C* **2014**, *118*, 17054 – 17059.
[28] E. M. Barea, M. Shalom, S. Giménez, I. Hod, I. Mora-Seró, A. Zaban, J. Bisquert, *J. Am. Chem. Soc.* **2010**, *132*, 6834 – 6839.
[29] S. Rühle, M. Greenshtein, S.-G. Chen, A. Merson, H. Pizem, C. S. Sukenik, D. Cahen, A. Zaban, *J. Phys. Chem. B* **2005**, *109*, 18907 – 18913.
[30] J. P. Bosco, S. B. Demers, G. M. Kimball, N. S. Lewis, H. A. Atwater, *J. Appl. Phys.* **2012**, *112*, 093703.
[31] S. W. Boettcher, E. L. Warren, M. C. Putnam, E. A. Santori, D. Turner-Evans, M. D. Kelzenberg, M. G. Walter, J. R. McKone, B. S. Brunschwig, H. A. Atwater, N. S. Lewis, *J. Am. Chem. Soc.* **2011**, *133*, 1216 – 1219.
[32] B. Seger, T. Pedersen, A. B. Laursen, P. C. K. Vesborg, O. Hansen, I. Chorkendorff, *J. Am. Chem. Soc.* **2013**, *135*, 1057 – 1064.
[33] D. R. Gamelin, *Nat. Chem.* **2012**, *4*, 965 – 967.
[34] C. Du, X. Yang, M. T. Mayer, H. Hoyt, J. Xie, G. McMahon, G. Bischoping, D. Wang, *Angew. Chem. Int. Ed.* **2013**, *52*, 12692 – 12695; *Angew. Chem.* **2013**, *125*, 12924 – 12927.
[35] J. A. Turner, *J. Chem. Educ.* **1983**, *60*, 327.
[36] M. Butler, *J. Appl. Phys.* **1977**, *48*, 1914 – 1920.
[37] M. S. Faber, R. Dziedzic, M. A. Lukowski, N. S. Kaiser, Q. Ding, S. Jin, *J. Am. Chem. Soc.* **2014**, *136*, 10053 – 10061.
[38] E. J. Popczun, J. R. McKone, C. G. Read, A. J. Biacchi, A. M. Wiltrout, N. S. Lewis, R. E. Schaak, *J. Am. Chem. Soc.* **2013**, *135*, 9267 – 9270.
[39] T. W. Kim, K.-S. Choi, *Science* **2014**, *343*, 990 – 994.

